Numerical Investigation of Cyclic Behavior of Angled U-shaped Yielding Damper on Steel Frames

Kambiz Cheraghi[1*], Mehrzad TahamouliRoudsari[2], Sasan Kiasat[3], Javad Esfandiari[2]

[1] Department of Civil Engineering, Faculty of Engineering, Razi University, Kermanshah 6714473421, Iran
[2] Department of Civil Engineering, Kermanshah Branch, Islamic Azad University, Kermanshah 6714473421, Iran
[3] Department of Civil and Environmental Engineering, AmirKabir University, Tehran 6714312312, Iran
* Corresponding author, e-mail: kambiz.cheraghi@gmail.com

Abstract

Yielding dampers are often selected as a cost-effective solution for improving steel structures compared to other energy dissipation systems. The objective of this research study was to investigate the cyclic behavior of the angled U-shaped yielding damper (AUSYD) on a steel frame using numerical method. The numerical model was first verified using two experimental samples. Next, the influence of the number of dampers on the cyclic behavior of the steel frame was examined. The parametric model outcomes included energy dissipation, elastic stiffness, strength, and equivalent viscous damping ratio (EVDR). Additionally, an analytical equation was proposed for calculating the ultimate strength of the AUSYD, which correlated well with the experimentally obtained results. The study findings revealed that the increase in elastic stiffness and strength of the frame equipped with the AUSYD was nearly equivalent to the sum of the elastic stiffness and strength of the bare frame and its supplementary dampers. Furthermore, the results showed that models with 8 to 12 dampers had comparable energy dissipation and EVDR. Adding 8 dampers to the frame increased the energy dissipation and damping coefficient of the frame by 42% and 67%, respectively.

Keywords

angled U-shape yielding damper, cyclic behavior, energy dissipation, numerical analysis

1 Introduction

Protecting humans from nature's forces is a primary goal when building structures. Methods to lessen structural harm from outside stresses are constantly evolving. Techniques to mitigate damage from natural events that are hard to forecast, like quakes, are also emerging [1, 2]. Earthquake design involves earthquake resistance, earthquake isolation [3], and earthquake damping to craft buildings that are safe during temblors. Quake resistance allows a structure to directly absorb seismic energy, protecting lives in strong quakes, but severe residual warping due to the inelastic behavior of the building results in enormous societal costs and environmental pollution from demolition. Quake isolation is the best way to avoid earthquake harm by separating a structure from the ground, making it untouched by quakes. However, quake isolation is difficult to apply to many structures as seismic isolator expenses can be prohibitive. Finally, quake damping permits damping devices, not the building, to absorb seismic energy. Damping apparatuses can be split into active

and passive control systems. The active control system is relatively pricey and complex since it demands several mechanical contraptions. On the other hand, the passive control system is relatively simple and economical, and it can easily be swapped when retrofitting structures after a quake. For these reasons, passive control systems are widely used in constructed structures [4–7].

Yielding dampers provide a suitable option for retrofitting steel and concrete frames. Researchers have conducted extensive studies on reinforcing concrete and steel frames with yielding dampers. TahamouliRoudsari et al. [8] conducted two numerical studies to investigate the effects of added damping and Stiffness (ADAS) and triangular Added Damping and Stiffness (TADAS) [9] dampers on the seismic behavior of reinforced concrete moment frames. Using 48 calibrated models and pushover analysis, they analyzed the impact of ADAS plates and axial loads on parameters such as stiffness, strength, energy dissipation, and ductility. They also experimentally tested

a retrofitted frame with TADAS dampers and utilized calibrated models to assess the influence of TADAS damper quantity and axial force on strength, stiffness, and ductility. The findings revealed an optimal response when the retrofitted frame's shear strength reached triple the initial capacity, and excessive axial compression significantly reduced energy dissipation and ductility. Ghaedi et al. [10] evaluated a new bar damper (BD) for semi-rigid frames. The BD consists of bars between plates dissipating energy through plastic deformation. Pushover analysis compared BD-equipped frames to bare frames, providing stress distribution insights. Cyclic displacement tests were also conducted on frames with and without BDs under actuator limits. Finite element models validated via experimental results showed BD devices enhanced frame strength, stiffness, damping, and energy dissipation. Cheraghi et al. [11] used ABAQUS to analyze a steel frame with low-yield steel yielding dampers (LYDs) through 40 pushover simulations. Effects of LYD quantity and column axial force were evaluated. Force-displacement curves were obtained to assess frame seismic parameters. Analytical relationships and contour plots were derived for strength and stiffness calculations. Results demonstrated LYDs improved seismic behavior, with optimal performance at 3.25 times bare frame stiffness and 0.13 times yield strength for all LYDs. Mahmoudi et al. [12] proposed a smaller cross-section shear link to dissipate energy and prevent end flexural yielding in beams. Experiments showed that a hybrid frame (HF) with the shear link had twice the ductility of a moment frame, with similar stiffness and strength. A verified numerical model expanded the new design concept. The effect of using U-shaped damper [13–15] ADAS and comb-teeth metallic dampers [16] has also been suggested for retrofitting steel frames due to their ability to improve seismic behavior. Merczel et al. [17] examine the weak story behavior and collapse of diagonally concentrically braced frames designed according to Eurocode 8. The study emphasizes understanding the nature and development of weak story behavior to improve design procedures. Additionally, the authors propose supplementary conditions based on plastic analysis to prevent weak story occurrences and enhance designs beyond Eurocode 8 provisions.

Fig. 1 illustrates the suggested location of the yield damper, as mentioned in several studies [14, 18–20]. The angled U-shaped yielding damper (AUSYD) reduces force on the steel frame in the "y" direction. However, the impact of using this damper and its quantity on the structure's cyclic behavior is unknown. This research

conducted parametric studies to analyze the effect of different AUSYD quantities on the steel frame, providing insights on energy dissipation, ultimate strength, elastic stiffness, and damping coefficient. Moreover, an analytical equation was developed to calculate the ultimate strength of the damper, which exhibited strong agreement with experimental results. The research focused on a one-story, one-span steel frame as the investigative model. Furthermore, the displacement-control approach was utilized for the analysis of the models.

2 Verification of numerical models
2.1 verification of AUSYD
In this section, the numerical model of AUSYD was verified. ABAQUS software was used to analyze the models. In the same way, the experimental sample of Kim and Kim [4] was used, which dimensions are shown in Fig. 2(a). The model investigated in this research includes 4 AUSYD numbers. The loading of this experimental sample was done cyclically. Rotation was not observed at the connections in the experimental specimen, with yielding occurring only in the width and length of the AUSYD. Fig. 2(b) shows the deformation of the experimental sample at the maximum displacement of 15 mm.

The AUSDs, bolts, and connection plates were simulated using C3D8I element and Static General solver of ABAQUS. Mesh sensitivity analysis was done with a discretization
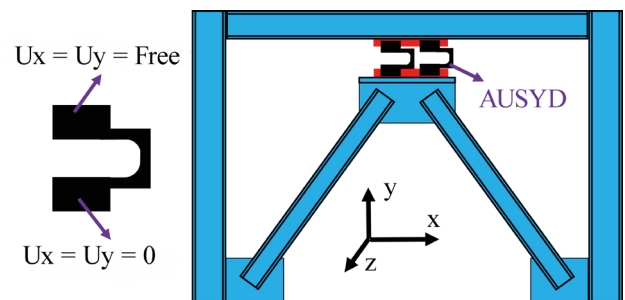

Fig. 1 location of the damper in the frame

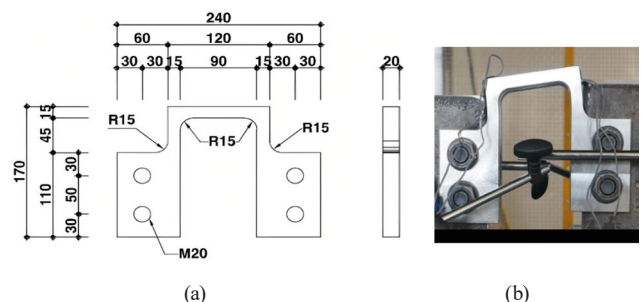(a)   (b)

Fig. 2 (a) Experimental sample dimensions, (b) deformation of the dampers [4]

size of 4 mm. No slippage was observed between the plates during loading with a coefficient of friction of 0.6 assumed between all members of the model. The presence of geometric imperfection did not significantly affect the results of the numerical model and was therefore disregarded. In the representation of the nonlinear geometric characteristics of materials, consideration was given to the inclusion of strain hardening and significant deformations in these components. Analysis of finite element models was carried out utilizing nonlinear static (General Static) and Newton-Raphson techniques. Fig. 3(b) illustrates the von Mises stress contour of the model at the end of loading, along with the boundary conditions and meshing of the model. The highest stress is observed to be concentrated in the dampers.
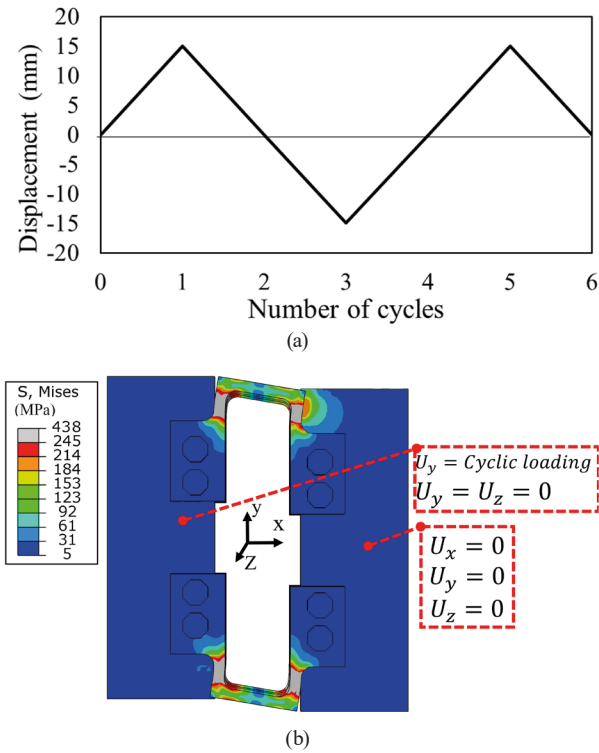

(a)

(b)

Fig. 3 (a) Loading history, (b) stress contour of the numerical model at maximum displacement

During the cyclic loading, the internal forces in the damper are illustrated in Fig. 4. The maximum moment in the damper is observed to be equal to PL/2. By equating this maximum moment to the plastic moment, it is possible to calculate the strength of the damper. The strength is determined by using Eq. (1), where "b" represents the thickness of the plate and is the maximum stress of the damper (420 GPa) [4]. The remaining parameters can be found in Fig. 4.

$$P_u = \frac{bt^2}{2L}\sigma_u = \frac{20 \times 15^2}{2 \times 115} \times 0.42 = 9kN \tag{1}$$

To simulate the hardening behavior of the steel, the Chaboche yield criterion [21, 22] was utilized. Fig. 5 illustrates the yield surface, which accounts for nonlinear isotropic and kinematic hardening. The Eqs. (2) and (3) describe the isotropic and kinematic hardening, respectively.

$$\sigma^0 = \sigma^0 \big|_0 + Q_\infty (1 - e^{-m \times \tilde{\varepsilon}_p}) \tag{2}$$

$$\alpha = \frac{C}{\gamma}(1 - e^{-\gamma \times \varepsilon_p}) \tag{3}$$

The force-displacement outcomes of the numerical model are displayed in Fig. 6, and they are compared with the experimental results. The comparison reveals that both models yield similar results with satisfactory precision. The numerical model effectively predicts the cyclic parameters of the damper.
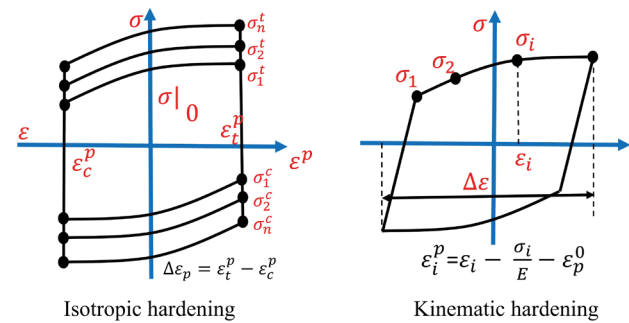

Isotropic hardening   Kinematic hardening

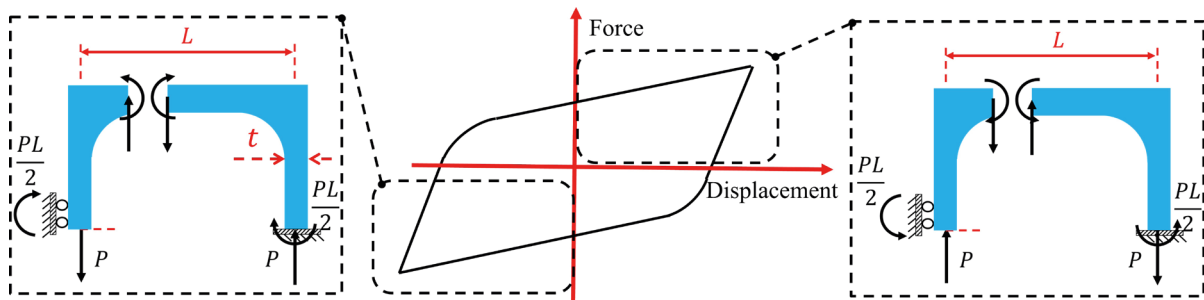**Fig. 5** Chaboche's model for isotropic and kinematic hardening [21, 22]

Fig. 4 Internal forces of the damper during cyclic loading
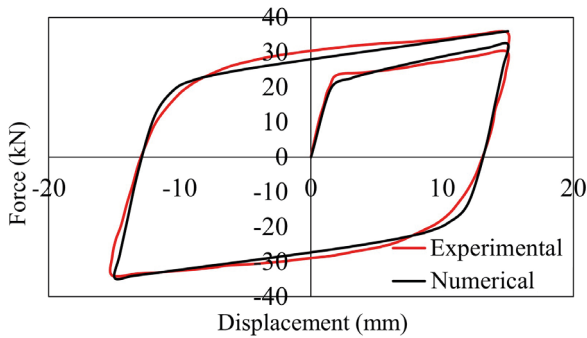
Fig. 6 Comparison of numerical and experimental results

2.2 Verification of steel frame

To check the accuracy of the numerical model, the steel frame tested by Hsu and Halim [23] was used in this part of the study. Fig. 7(a) shows the details of this steel frame. In this frame, the connections are rigid, and the connection of the column to the ground is hinged.

The shell element (S4R) was employed for numerical modeling of all frame members of steel frame. Non-linear static analysis with a displacement-control technique was utilized for lateral loading. Mesh dimensions of the frame were set to 20 mm based on sensitivity analysis. The meshed model of the frame and the considered boundary conditions can be seen in Fig. 7(b). Figs. 7(c) and 7(d) show the stress contour of the models of this research and the experimental sample [23]. It can be seen that the yield zones are the same in the two models.

Fig. 8 shows the comparison of the numerical and experimental results of the steel frame. It can be seen that they are close to each other with acceptable accuracy. Table 1 shows the results of three seismic parameters of experimental and numerical samples of steel frame and damper. In this table, stiffness (initial slope of the force-displacement curve), strength and energy dissipation (internal area of the residual loops) are shown. It can be seen that the obtained results are close to each other with acceptable accuracy and the results of the numerical model can be assured for more cases.
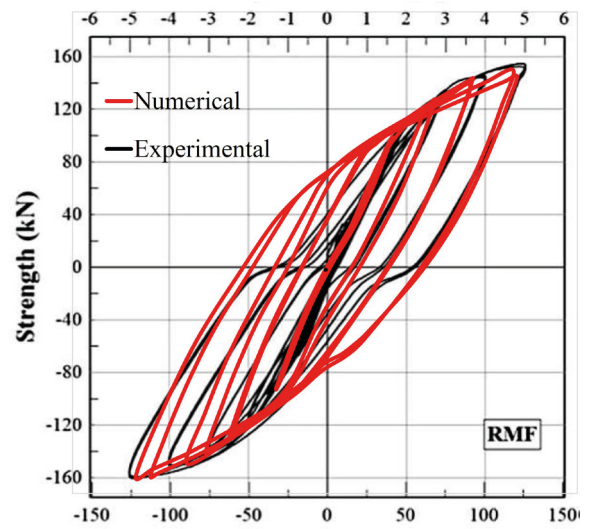

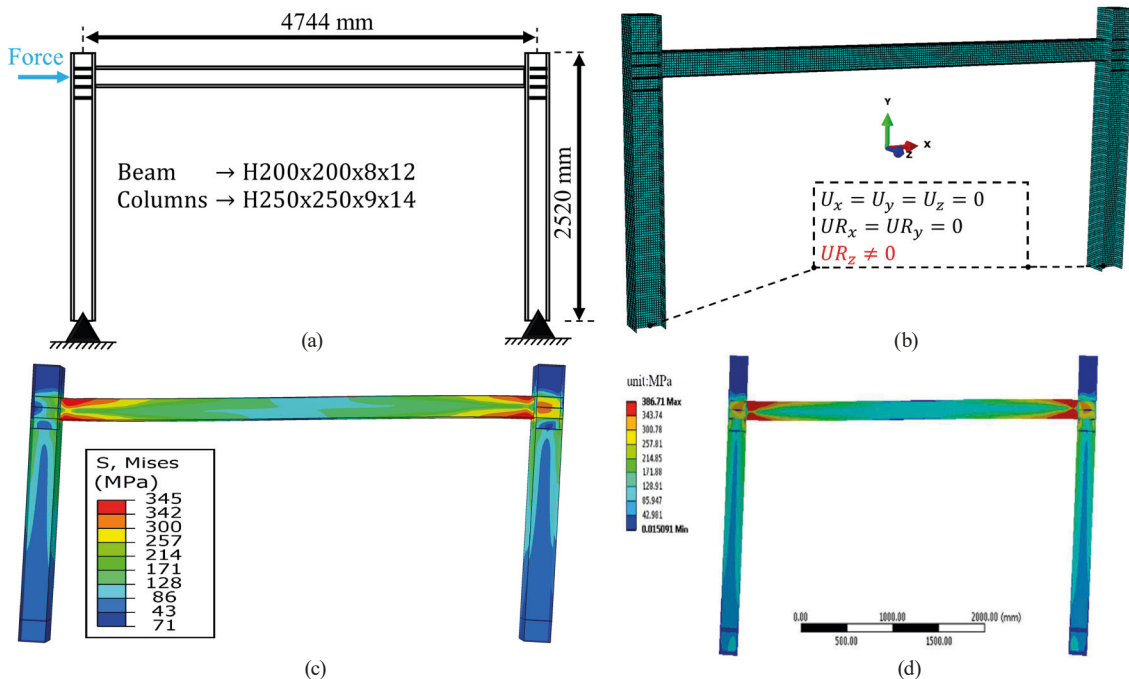**Fig. 8** Comparison of numerical and experimental hysteresis results

Fig. 7 (a) Characteristics of the experimental sample, (b) Boundary conditions of the numerical model, (c) Comparison of numerical and (d) experimental model stress [23]

Table 1 Comparison of numerical, experimental and analytical results of verification samples

| Parameters	AUSYD			Steel Frame	
	FEM	Exp. [4]	Ana.	FEM	Exp. [23]
Elastic stiffness (kN/mm)	15.3	15.2	-	2.43	2.38
Strength (kN)	36.1	36.2	36	152.1	154
Energy dissipation (kN.mm)	1826.5	1875.7	-	82325	77000

3 Parametric study

In this section, the main model was examined. The frame and specifications of the main model were considered as Fig. 9. The dimensions of the steel frame and dampers were considered equal to the verified models. The loading protocol of the model, according to the experimental sample of the steel frame, was considered as Fig. 10. All the specifications of the model were considered equal to the verified model. The following points were considered in the design of this model:

- All the connections were made in the numerical model with "Tie" constraint.
- The sections of braces were designed so that they do not buckle until the end of loading in any of the models.
- The dimensions of meshing were considered to be the same as the verified model. In the new model, the correctness of these meshing dimensions was also checked.
- The analysis of the models was done according to the control-displacement technique.
- After analyzing the models, their results were shown in Fig. 11.
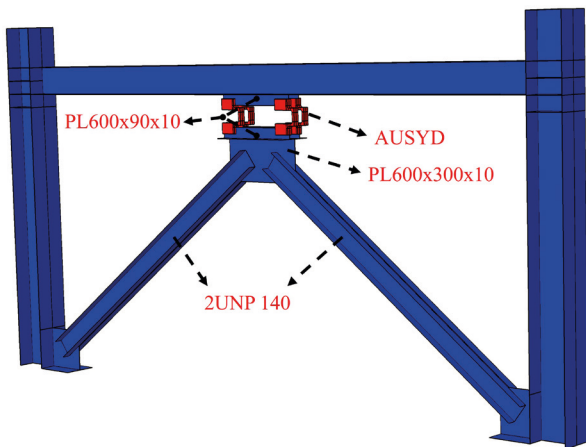
Fig. 9 Specifications of the main model
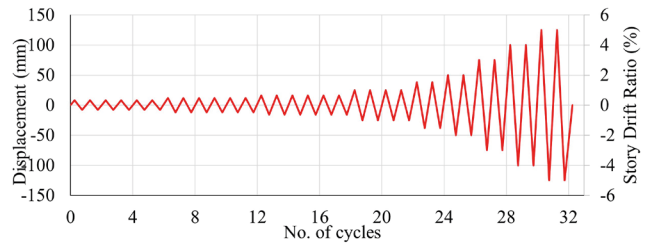
Fig. 10 Loading procedure applied in parametric models [23]
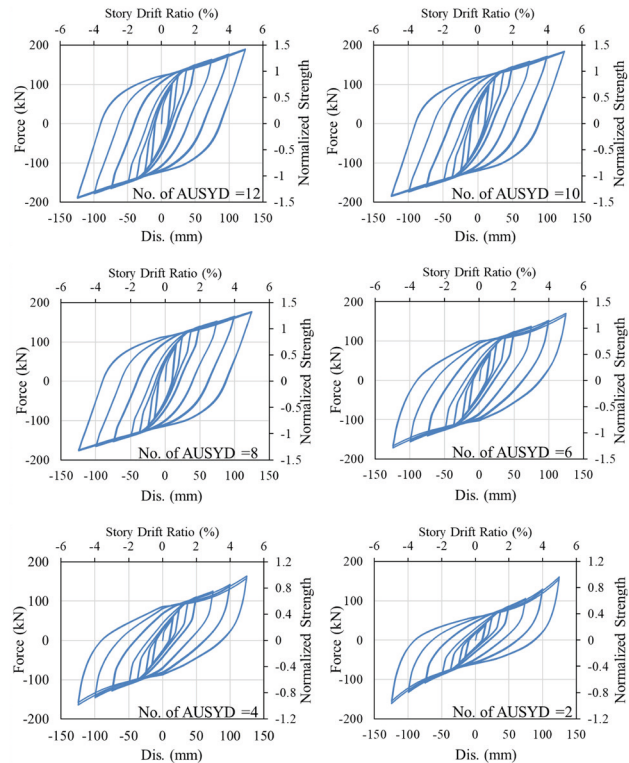
Fig. 11 Hysteretic loops of results for parametric models

Fig. 12(a) illustrates the energy dissipation of the models, normalized to the bare frame. It is evident that the curve exhibits a steep slope up to the use of eight dampers, after which it becomes relatively constant. On the other hand, Fig. 12(b) presents the cumulative energy dissipation of the models in relation to the displacement of the frame. It can be seen that in the models with 8 to 12 dampers, the results are almost close to each other and this parameter has decreased with the decrease in the number of dampers. Fig. 12(c) depicts a crucial design diagram for AUSYD-equipped frames. It illustrates normalized energy dissipation against stiffness relative to the bare frame. This diagram facilitates the calculation of energy dissipation increase based on the frame's stiffness ratio compared to the bare frame.
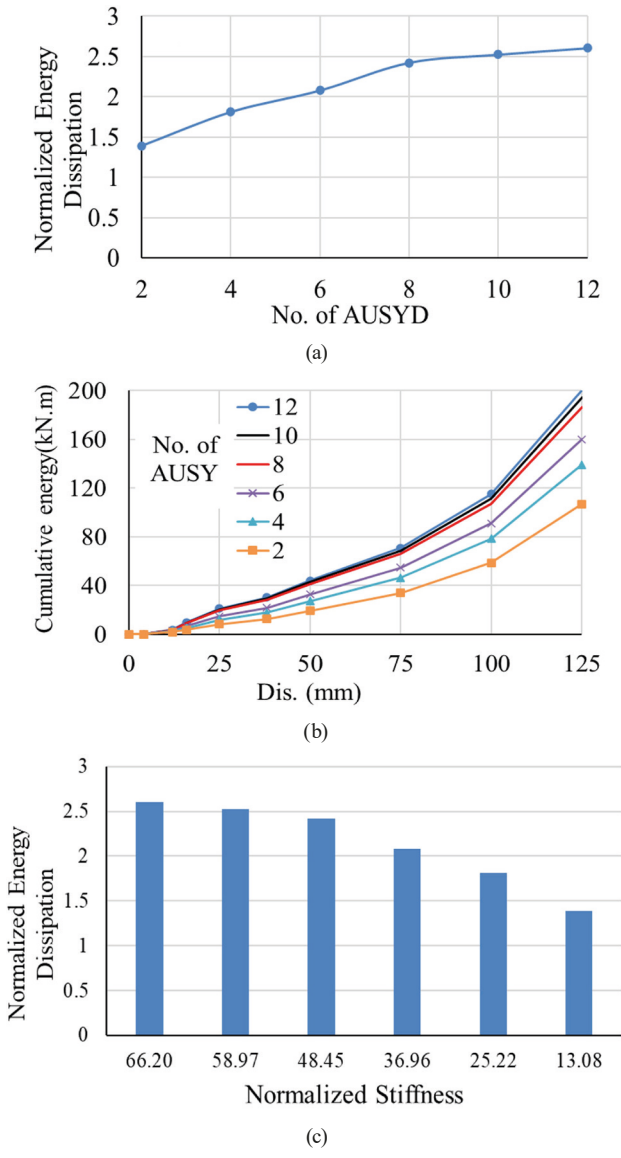
(a)

(b)

(c)

Fig. 12 (a) Normalized energy dissipation, (b) cumulative energy dissipation, (c) normalized energy dissipation versus normalized stiffness

Fig. 13(a) displays the normalized strength of the models with respect to the bare frame. It is apparent that the strength of the model increases almost linearly with an increase in the number of dampers. The model's strength can be determined by adding the strength of the bare frame to that of its supplementary dampers, as expressed in Eq. (4) where "n" denotes the number of dampers in the model. The results of this equation and numerical analysis are shown in Fig. 13(a). It can be seen that they are close to each other with acceptable accuracy. Fig. 13(b) shows the ultimate strength results of the models compared to its displacement.

$$P_u = P_{u,bare\ frame} + nP_{u,AUSYD} \tag{4}$$

Fig. 14 shows the effective stiffness of the frame versus to the number of its dampers. It can be seen that the rate of increase in the stiffness of the frame is almost linear with the increase in the number of dampers. The difference between numerical and analytical results in Figs. 13(a) and 14 is due to neglecting large deformations (second-order analysis). Since the displacement of the frame and dampers are the same. According to the law of springs, the total stiffness is equal to the sum of the stiffness of its members [24]. Therefore, according to Eq. (5), the stiffness of the frame can be calculated, which is equal to the sum of the stiffness of the bare frame and its dampers. Fig. 14 shows the results obtained from Eq. (5) and the numerical results, which can be seen to be reasonably close to each other.
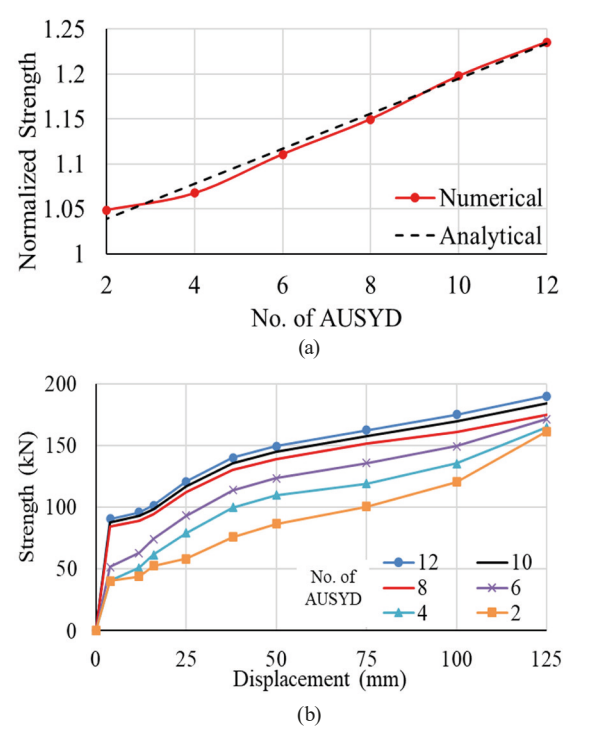
$$K_e = K_{e,bare\ frame} + nK_{e,AUSYD} \tag{5}$$

(a)

(b)

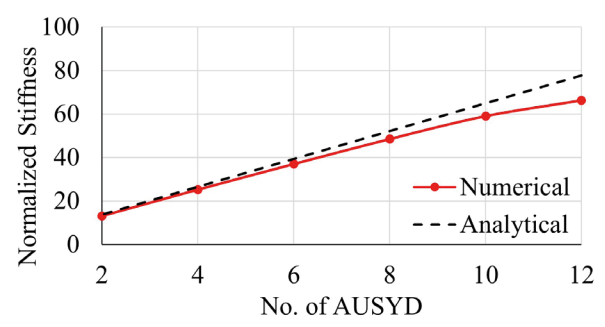**Fig. 13** Ultimate strength relative to the (a) number of dampers, (b) displacement of the frame

Fig. 14 Elastic stiffness of the frame

The equivalent viscous damping ratio (EVDR) is one of the essential seismic parameters of the model. This section assesses the influence of the number of dampers on this parameter. The EVDR can be determined based on Eq. (6) using the parameters from Fig. 15(a), with the final loop curve of the results illustrated in Fig. 15(b). Similarly, Fig. 15(c) represents the EVDR of the models in which the EVDR is normalized to the bare frame. The figure reveals that the EVDR increases as the number of dampers rises, with the curve exhibiting a steep slope until eight dampers are used, after which the rate of increase becomes nearly constant.

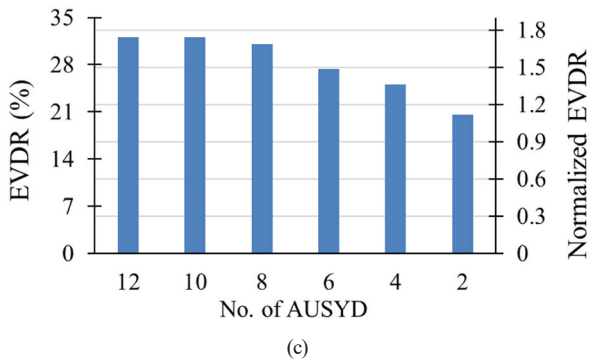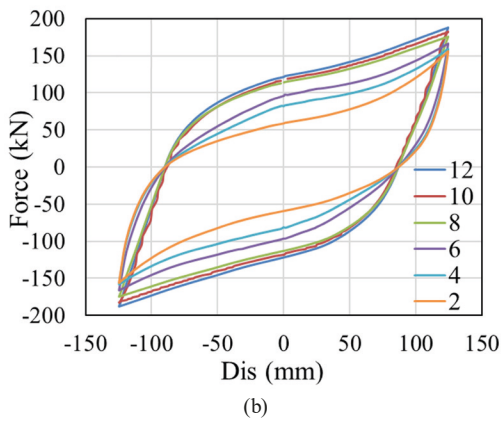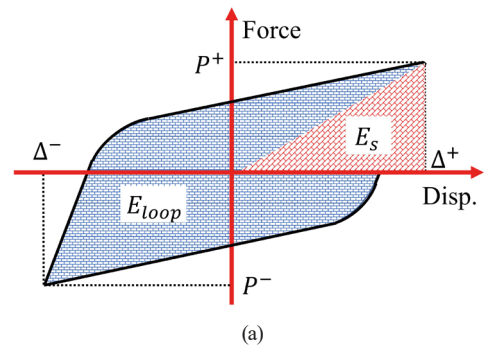$$\xi = \frac{E_{loop}}{4\pi E_s} \tag{6}$$

In this section, the stress contour of the steel frame during loading was investigated. One of the important points in the design of structures equipped with a yielding damper is that the yielding damper should yield before the main members of the structure. In the numerical model of the present research, according to Fig. 16, it was observed that yielding occurred in the parallel members of damper during loading. Because the stress distribution in the models was almost the same. Only the results of one of the models are presented.

4 Conclusions

This study conducted parametric investigations on the influence of AUSYD on a steel moment frame. The numerical model was calibrated based on the results of two experimental samples, after which the number of AUSYD was varied from 2 to 12. An analytical equation was also introduced to determine the ultimate strength of the damper, which demonstrated excellent agreement
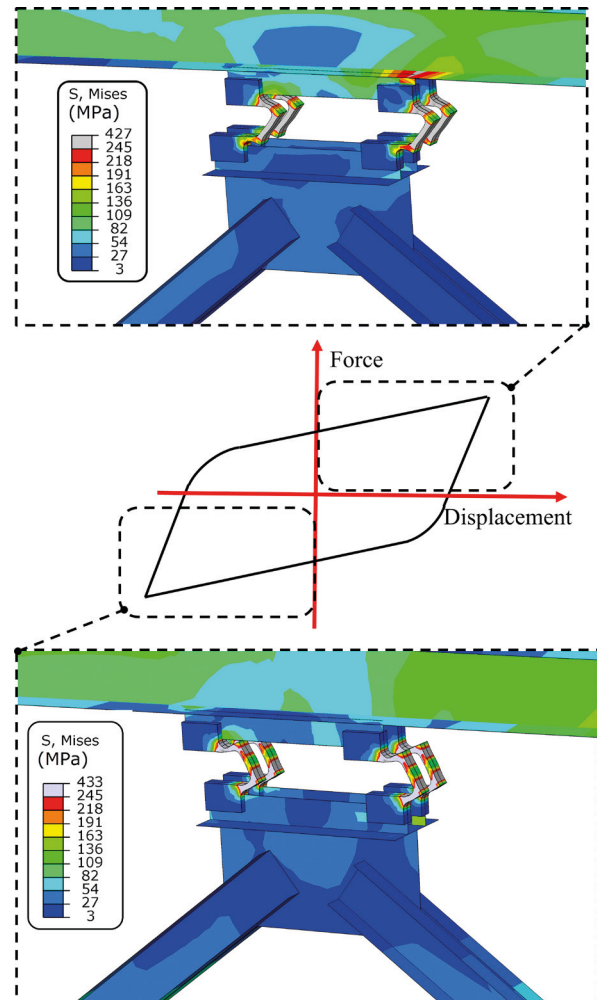

Fig. 15 (a) Schematic of the hysteretic loop, (b) The final loop results, (c) numerical results of EVER

Fig. 16 Stress distribution of the model

with the experimental outcomes. The resulting parametric model included energy dissipation, ultimate strength, effective stiffness and EVDR. The results of the numerical analysis are as follows:

- The stiffness and ultimate strength of the frame equipped with AUSYD displayed an almost linear rate of increase in relation to the number of added dampers. Equations were formulated to calculate these two parameters based on the summation of the strength and stiffness of the bare frame and its dampers, which demonstrated good conformity with the numerical findings.
- Regarding energy dissipation, the total dissipated energy of the frame increased with an increase in the number of dampers. The rate of energy dissipation

increment was shown to be high up to eight dampers, after which it became nearly constant. The addition of eight dampers increased the strength of the bare frame by 2.42 times.

- Adding the number of dampers increased the EVDR of the frame. So that similar to the energy loss, the rate of increase was high up to 8 dampers and after that it was almost constant. Adding eight AUSYDs increased the frame's EVDR by 75%.
- The analysis demonstrated that, for cost-effectiveness, a frame equipped with eight dampers was optimal. In this configuration, the ratio of the damper stiffness to the bare frame was 51, and no significant effect on the results was observed with an increase in the number of dampers.

References

[1] El Ouni, M. H., Ben Kahla, N., Ahmed, M., Islam, S., Ayed, H., Khedher, K. M. "Comparative Study of Different Active Control Systems of High Rise Buildings under Seismic Excitation", Periodica Polytechnica Civil Engineering, 63(4), pp. 1092–1102, 2019.
https://doi.org/10.3311/PPci.14367

[2] Merczel, D. B., Somja, H., Aribert, J.-M., Lógó, J. "On the behaviour of concentrically braced frames subjected to seismic loading", Periodica Polytechnica Civil Engineering, 57(2), pp. 113–122, 2013.
https://doi.org/10.3311/PPci.7167

[3] Dao, N. D. "Simple Equations for Predicting Maximum Displacement of Isolation Systems Using Lead Rubber Bearings", Periodica Polytechnica Civil Engineering, 66(3), pp. 843–852, 2022.
https://doi.org/10.3311/PPci.19894

[4] Kim, S.-W., Kim, K.-H. "Evaluation of structural behavior of hysteretic steel dampers under cyclic loading", Applied Sciences, 10(22), 8264, 2020.
https://doi.org/10.3390/app10228264

[5] Mohebbi, M., Dabbagh, H. R., Shakeri, K. "Optimal Design of Multiple Tuned Liquid Column Dampers for Seismic Vibration Control of MDOF Structures", Periodica Polytechnica Civil Engineering, 59(4), pp. 543–558, 2015.
https://doi.org/10.3311/PPci.7645

[6] Hosseinaei, S., Ghasemi, M. R., Etedali, S. "Optimal Design of Passive and Active Control Systems in Seismic-excited Structures Using a New Modified TLBO", Periodica Polytechnica Civil Engineering, 65(1), pp. 37–55, 2021.
https://doi.org/10.3311/PPci.16507

[7] Hojat Jalali, H., Fahimi Farzam, M. "Inerter-Connected Double Tuned Mass Damper for Passive Control of Buildings under Seismic Excitation", Periodica Polytechnica Civil Engineering, 66(2), pp. 421–432, 2022.
https://doi.org/10.3311/PPci.19638

[8] TahamouliRoudsari, M., Cheraghi, K., Habibi, M. R. "Investigation of retrofitting RC moment resisting frames with ADAS yielding dampers", Asian Journal of Civil Engineering, 20(1), pp. 125–133, 2019.
https://doi.org/10.1007/s42107-018-0092-6

[9] TahamouliRoudsari, M., Cheraghi, K., Aghayari, R. "Investigating the Retrofit of RC Frames Using TADAS Yielding Dampers", Structural Durability & Health Monitoring, 16(4), pp. 343–359, 2022.
https://doi.org/10.32604/sdhm.2022.07927

[10] Ghaedi, K., Javanmardi, A., Ibrahim, Z., Gordan, M., Rashid, R. S. M., Khatibi, H., Vaghei, R. "Experimental and numerical studies on the cyclic performance of structural frames equipped with bar dampers", Structures, 50, pp. 707–722, 2023.
https://doi.org/10.1016/j.istruc.2023.02.070

[11] Cheraghi, K., Tavana, M. H., Aghayari, R. "Investigating the Effect of Low-Yield Yielding Dampers on the Seismic Behavior of Steel Frames", Periodica Polytechnica Civil Engineering, 2023.
https://doi.org/10.3311/PPci.21804

[12] Mahmoudi, F., Dolatshahi, K. M., Mahsuli, M., Nikoukalam, M. T., Shahmohammadi, A. "Experimental study of steel moment resisting frames with shear link", Journal of Constructional Steel Research, 154, pp. 197–208, 2019.
https://doi.org/10.1016/j.jcsr.2018.11.027

[13] Cheraghi, K., TahamouliRoudsari, M., Kiasat, S. "Numerical and analytical investigation of U-shape dampers and its effect on steel frames", Structures, 55, pp. 498–509, 2023.
https://doi.org/10.1016/j.istruc.2023.06.037

[14] Ebadi Jamkhaneh, M., Ebrahimi, A. H., Shokri Amiri, M. "Experimental and Numerical Investigation of Steel Moment Resisting Frame with U-Shaped Metallic Yielding Damper", International Journal of Steel Structures, 19(3), pp. 806–818, 2019.
https://doi.org/10.1007/s13296-018-0166-z

[15] Bagheri, S., Barghian, M., Saieri, F., Farzinfar, A. "U-shaped metallic-yielding damper in building structures: Seismic behavior and comparison with a friction damper", Structures, 3, pp. 163–171, 2015.
https://doi.org/10.1016/j.istruc.2015.04.003

[16] Garivani, S., Aghakouchak, A. A., Shahbeyk, S. "Seismic Behavior of Steel Frames Equipped with Comb-Teeth Metallic Yielding Dampers", International Journal of Steel Structures, 19(4), pp. 1070–1083, 2019.
https://doi.org/10.1007/s13296-018-0188-6

[17] Merczel, D. B., Aribert, J.-M., Somja, H., Hjiaj, M. "Plastic analysis-based seismic design method to control the weak storey behaviour of concentrically braced steel frames", Journal of Constructional Steel Research, 125, pp. 142–163, 2016.
https://doi.org/10.1016/j.jcsr.2016.05.008

[18] Bagheria, S., Hadidi, A., Alilou, A. "Heightwise Distribution of Stiffness Ratio for Optimum Seismic Design of Steel Frames with Metallic-Yielding Dampers", Procedia Engineering, 14, pp. 2891–2898, 2011.
https://doi.org/10.1016/j.proeng.2011.07.364

[19] Maleki, S., Mahjoubi, S. "Dual-pipe damper", Journal of Constructional Steel Research, 85, pp. 81–91, 2013.
https://doi.org/10.1016/j.jcsr.2013.03.004

[20] Zheng, J., Li, A., Guo, T. "Analytical and experimental study on mild steel dampers with non-uniform vertical slits", Earthquake Engineering and Engineering Vibration, 14(1), pp. 111–123, 2015.
https://doi.org/10.1007/s11803-015-0010-9

[21] Chaboche, J. L. "A review of some plasticity and viscoplasticity constitutive theories", International Journal of Plasticity, 24(10), pp. 1642–1693, 2008.
https://doi.org/10.1016/j.ijplas.2008.03.009

[22] Chaboche, J.-L., Kanouté, P., Azzouz, F. "Cyclic inelastic constitutive equations and their impact on the fatigue life predictions", International Journal of Plasticity, 35, pp. 44–66, 2012.
https://doi.org/10.1016/j.ijplas.2012.01.010

[23] Hsu, H.-L., Halim, H. "Improving seismic performance of framed structures with steel curved dampers", Engineering Structures, 130, pp. 99–111, 2017.
https://doi.org/10.1016/j.engstruct.2016.09.063

[24] Hibbeler, R.C., Tan, K.-H. "Structural analysis", Prentice Hall. 2005. ISBN 0131976419